

A reexamination of the low-temperature crystal structure of the *p*-*tert*-butylcalix[4]arene–toluene inclusion compound. Differences in spatial averaging with Cu and Mo $K\alpha$ radiation

Gary D. Enright,* Eric B. Brouwer, Konstantin A. Udachin, Christopher I. Ratcliffe and John A. Ripmeester

Steacie Institute for Molecular Sciences,
National Research Council Canada, Canada

Correspondence e-mail: gary.enright@nrc.ca

Received 3 September 2002

Accepted 14 October 2002

The low-temperature crystal structure of the *p*-*tert*-butylcalix[4]arene–toluene inclusion compound, $C_{44}H_{56}O_4 \cdot C_7H_8$, exhibits significant guest-induced distortion of the host calixarene molecule. This distortion persists long enough to establish a correlation in the orientation of guests in adjacent host molecules. Remarkably, the space group and unit cell that best describe the structure appear to depend on the wavelength of the incident radiation. This behaviour appears to arise from spatial averaging over the different scattering volumes required to establish the diffraction peaks.

1. Introduction

In our initial low-temperature structural studies of the toluene inclusion compound of *p*-*tert*-butylcalix[4]arene (*t*BC) the X-ray data were collected on an Enraf–Nonius CAD-4 diffractometer with Cu $K\alpha$ radiation (Brouwer *et al.*, 1996). A puzzling aspect of these studies was the appearance of transient diffraction peaks, half-integral in *h* and *k*. These peaks, which corresponded to a tetragonal unit cell with double the volume of that used in the refinement, were attributed to a transient superstructure that arises from a strong correlation in the alignment of guest molecules in adjacent unit cells. As these superlattice peaks only persisted for a few hours immediately after cooling, we were unable to collect a full data set. We have recollected the low-temperature data with a Siemens SMART CCD diffractometer using Mo $K\alpha$ radiation. The weak superlattice peaks are now persistent. Remarkably, the unit cell and space group that best fit the sets of diffraction data depend on the wavelength of the incident radiation. The differences in the derived structures arise from the spatial averaging over the different scattering volumes that are needed to establish the diffraction peaks ($V_{Cu}/V_{Mo} \simeq 10$).

The room-temperature structure of *t*BC–toluene has been determined by Andreeti *et al.* (1979). In their refinement model the toluene guest molecule was found to lie along a fourfold crystallographic axis with its methyl group inserted into the conical cavity of the calixarene host molecule. In order to satisfy the fourfold crystallographic symmetry, the guest molecules were disordered over two equivalent sites. In addition, the *t*-butyl groups of the host molecule were reported to be disordered (77:23) over two sites.

Solid-state ^{13}C NMR studies indicated that at room temperature the toluene guest rapidly reorients between all equivalent guest sites. However, below 248 K a splitting of many of the ^{13}C calixarene resonance lines indicated a transition to a lower-symmetry host lattice (Facey *et al.*, 1993). Differential scanning calorimetry (DSC) has also provided evidence of a broad exothermic peak at 248 K, which indicates a phase transition. However the crystal structure initially

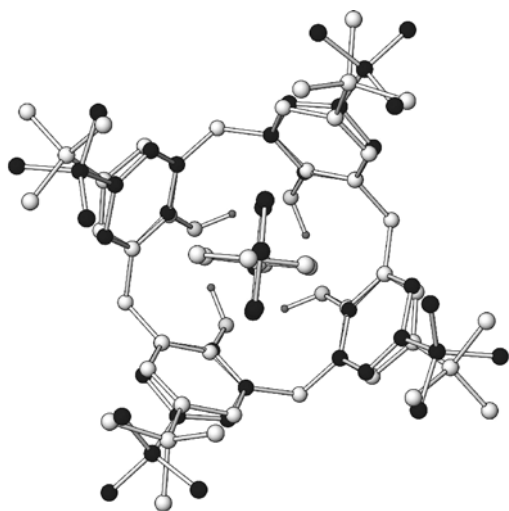


Figure 1
The *t*BC–toluene structure determined at 151 K (with Cu radiation). The guest-induced distortion of the *t*BC host molecule is evident.

determined at 151 K (with Cu radiation) exhibited the same high-symmetry space group ($P4/n$) as at room temperature (Brouwer *et al.*, 1996). Upon refinement, new structural details, which correspond to a lowering of the local symmetry, were resolved. The long axis of the toluene guest was observed to be tilted off the host fourfold axis of symmetry by $\sim 11.5^\circ$, and this tilting resulted in four equivalent overlapping guest sites (related by 90° rotations about the host molecule's fourfold axis). The *t*-butyl disorder could now be interpreted as a guest-induced distortion of the host calixarene molecule, where this distortion appears as a 50:50 disorder. Two opposing aromatic rings of the calixarene pivot outward, and the attached *t*-butyl group rotates about its local axis of symmetry. This distortion is probably correlated with the orientation of the toluene guest, as steric effects induce the flexible upper rim to distort away from the toluene guest as depicted in Fig. 1. The apparent high (tetragonal) symmetry of the structure determined from X-ray diffraction is due to spatial averaging over many sites occupied by the distorted (lower-symmetry) calixarene molecules. The agreement factors for the room-temperature structure were greatly improved by using the twinned structural model derived for the 151 K data.

2. Experimental

The crystallographic data for the low-temperature Cu measurements (I), the room-temperature Cu measurements (II) and the low-temperature Mo measurements (III) are summarized in Table 1.¹ Structure (III) was initially solved in the space group $P4$ and refined to an overall agreement factor (R_1) of $\sim 7\%$. However, the observed structural details and

¹Supplementary data for this paper are available from the IUCr electronic archives (Reference: AN0621). Services for accessing these data are described at the back of the journal.

Table 1

Crystallographic data for *t*BC–toluene at 151, 296 and 173 K.

Compound	(I)	(II)	(III)
Empirical formula	$C_{11}H_{14}O(C_7H_8)_{0.25}$	$C_{11}H_{14}O(C_7H_8)_{0.25}$	$C_{44}H_{56}O_4(C_7H_8)$
Temperature (K)	151	296	173
Wavelength (Å)	1.54056	1.54056	0.70926
Space group	$P4/n$	$P4/n$	$P2/c$
Unit-cell dimensions (Å)	$a = 12.5540$ (3) $c = 13.7665$ (2)	$a = 12.7726$ (2) $c = 13.8068$ (5)	$a = 17.8141$ (17) $b = 13.8901$ (13) $c = 17.8060$ (18)
β (°)			89.91 (1)
Volume	2169.64 (8)	2252.43 (9)	4405.9 (10)
Z	8	8	4
μ (mm ⁻¹)	0.50	0.49	0.07
2θ maximum	139.5	139.9	57.4
Reflections/unique	4693/2049	4452/2157	51325/11537
R_{merge}	0.013	0.014	0.042
Reflections $I > 2.5\sigma(I)$	1727	1385	
Reflections $F_o > 4\sigma(F_o)$			9480
R indices $I > 2.5\sigma(I)$	$R_1 = 0.051$ $R_w = 0.077$	$R_1 = 0.046$ $R_w = 0.063$	
R indices $F_o > 4.0\sigma(F_o)$			$R_1 = 0.051$ $R_w = 0.122$
Goodness-of-fit	2.73	2.24	1.09
Maximum Δ/σ	0.044	0.064	0.008
Residual density (e Å ⁻³)	-0.22, +0.25	-0.22, +0.12	-0.25, +0.31

packing were complex and difficult to fully understand as there appeared to be alternating layers of ordered twofold and disordered fourfold *t*BC cavities. Examination of the agreement between equivalents (R_{merge}) for different possible Laue groups indicated a slight preference for monoclinic ($P112/m$) over tetragonal ($P4/m$ symmetry) so the structure was transformed to *b*-axis unique and solved as a highly twinned monoclinic structure with space group $P2$. After the data had been checked for missed symmetry (*MISSYM*; Le Page, 1988) the space group $P2/c$ was indicated and the refinement was completed. The relationships between the lattice vectors **a**, **b** and **c** (of I and II) and the new lattice vectors **a'**, **b'** and **c'** (of III) are $\mathbf{a}' = \mathbf{a} + \mathbf{b}$, $\mathbf{b}' = \mathbf{c}$ and $\mathbf{c}' = \mathbf{a} - \mathbf{b}$. The twinning fraction was determined to be 0.425 (1). It is interesting to note that although both (I) and (II) can be successfully solved as twinned $P2/n$ (*c*-axis unique, with a twinning fraction of 0.50) the agreement factor does not improve despite a modest increase in the number of parameters. At the resolution of the present experiment (~ 0.82 Å) we cannot distinguish between a disordered $P4/n$ and a twinned $P2/n$ structural model for (I) and (II). All the structures were solved and refined initially with the *NRCVAX* suite of programs (Gabe *et al.*, 1989). For refinement of the twinned structures *SHELXTL* (Sheldrick, 2001) was employed.

3. Discussion

The low-temperature structure that is derived from the data collected with Mo $K\alpha$ radiation clearly shows the guest-induced distortion of the host molecules and confirms the correlation in the guest alignment in adjacent calixarene

molecules. The lattice appears to be metrically tetragonal with a unit-cell volume double that observed with Cu radiation, but the structure is best described as a highly twinned monoclinic lattice with *t*BC molecules centred on twofold axes. There are two crystallographically distinct *t*BC molecules, each with a toluene guest that is disordered over two equivalent sites (related by a 180° rotation about the calixarene's twofold axis of symmetry). There is no longer any *t*-butyl disorder in the calixarene host molecule. The packing of adjacent calixarene molecules in the *ab* plane perpendicular to the unique axis is shown in Fig. 2. The observed phase transition at 248 K can be associated with the onset of long-range order in the orientation of the guest molecules.

In all of the structures the calixarene host molecules are packed in layers perpendicular to the unique crystallographic axis, with the host molecules' bowl-shaped cavities directed alternately upwards and downwards from a common plane (which is located approximately at the midpoint of the C—O bonds at the base of the phenyl rings). For clarity Fig. 2 shows only the upward-pointing molecules. Circles mark the positions of the downward-pointing molecules. The packing motif is analogous to a checkerboard with each host molecule occupying a single square. Those molecules on black squares all point upward from a common base and those on the red squares (locations depicted by circles in Fig. 2) all point downward from the same common base. The bowl-shaped cavities are 'capped' by *t*-butyl C atoms from four surrounding host molecules in the next layer.

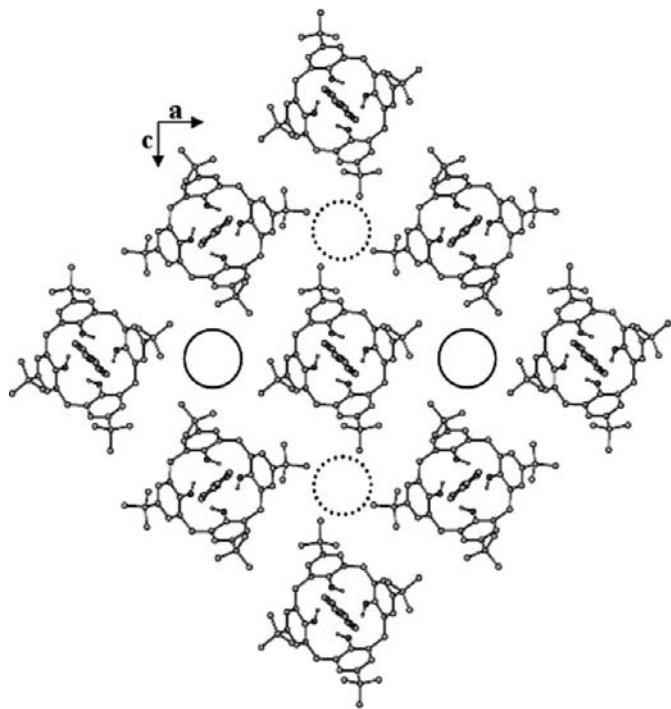


Figure 2
Packing of the *t*BC–toluene crystal as determined at 173 K with Mo radiation. The circles indicate the positions of the downward-facing *t*BC molecules.

Table 2
Parameters describing the guest–host positions.

D_1 and D_2 are the dihedral angles between the plane of the *t*BC phenyl units and the plane perpendicular to the unique twofold axes, D_3 is the dihedral angle for the plane containing the toluene guest, φ is the angle between the long axis of the toluene guest and the twofold axis, and d is the distance of the toluene methyl C atom above the base of the *t*BC cavity (as defined by the plane of the four O atoms).

	Calixarene host		Toluene guest		
	D_1 (°)	D_2 (°)	φ (°)	D_3 (°)	d (Å)
I	61.8	53.5	11.54	88.8	3.65
II	58.0	55.5	13.64	87.2	3.78
IIIa	61.7	54.8	7.75	88.0	3.83
IIIb	60.5	53.5	4.20	89.5	3.64

The reason for the two crystallographically distinct *t*BC molecules in (III) becomes clear upon a careful examination of Fig. 2. The downward-directed *t*BC cavities that are located in the layer directly above the dashed circles are 'capped' by four *t*-butyl C atoms that insert radially into the cavity, whereas the *t*BC cavities that are located above the solid circles are capped by eight C atoms that are directed more or less tangentially to the cavity. As a result, guests from opposing cavities in the next layer, that is, those guests located above the dashed circles, are restricted to lie closer to the axis of the *t*BC cavity than those guests located above the solid circles.

The presence of the guest molecule distorts the host cavity and lowers the local symmetry. In our refinements the distortion is modelled by 50:50 disorder (for I and II) or by dropping the Laue symmetry from tetragonal to monoclinic (for III). In both models the cavity symmetry drops from fourfold to twofold. The extent of the distortion can be seen by comparing the observed changes in the dihedral angles D_1 and D_2 (Table 2) between the plane of the phenyl units that form the walls of the cavity and the horizontal. The difference between D_1 and D_2 is a measure of the magnitude of the distortion. This induced distortion is greater at low temperatures where the steric interaction between the guest and the host is increased because of the thermal contraction of the unit cell. Also shown in Table 2 are three parameters that describe the guest position in the *t*BC cavity. φ is the angle between the long axis of the toluene guest and the twofold axis of the *t*BC cavity, D_3 is the dihedral angle between the plane containing the guest molecule and the plane perpendicular to the cavity axis, and d is the distance (in Å) above the base of the *t*BC cavity (as defined by the plane of the four O atoms) of the methyl C atom of the guest. In (III), the difference between the two distinct cavities (denoted by IIIa and IIIb) is clear. The guest in the restricted cavity (IIIb) is confined much closer to the axis of the *t*BC cavity (as discussed above).

The differences in the two low-temperature data sets can be simply explained. For a well defined diffraction peak to exist, the diffracted beam must be a plane wave. The lack of long-range order in the crystal will introduce random phase shifts across the diffracted beam. If these shifts occur on a scale length less than a few tens of λ_0 then the distorted wavefront

acquires curvature and leads to diffuse scattering. Therefore, Bragg peaks require a coherent scattering volume that scales as λ_0^3 and as a result Cu $K\alpha$ Bragg peaks are averaged over crystal domains with a volume that is ten times greater than that with Mo $K\alpha$.

4. Conclusions

It has been recognized that the techniques of solid-state NMR and X-ray diffraction provide complementary information about the crystalline structure. Solid-state CP/MAS (cross-polarization magic-angle spinning) NMR provides details of the local environment of the atomic nuclei whereas X-ray diffraction provides structural information that is spatially averaged over many unit cells. As discussed above, the scale length over which this averaging occurs will depend on the wavelength of the X-rays. In the present study the correlation in the guest orientation (and the accompanying distortion in the host *t*BC molecule) persists on a scale length that is long enough to produce Bragg peaks with Mo radiation but not long enough to produce Bragg peaks with Cu radiation except for a short time immediately after cooling. In this sense the information derived from the Mo diffraction data is intermediate between that derived from Cu diffraction data and that from CP/MAS NMR.

The observed time dependence of the superlattice peaks in the Cu $K\alpha$ experiments has to arise from a physical process that is independent of the wavelength. This fact suggests that there is a greater degree of long-range order present immediately after cooling and that this order extends through the coherent scattering volume that is required for Cu radiation but diminishes below this volume with time. Perhaps stresses induced by the rapid cooling process are relieved at the domain boundaries of the highly twinned crystal. The average domain size, which is large enough to produce the superlattice peaks with Cu radiation immediately upon cooling, decreases in time as the stresses are annealed out.

References

- Andreeti, G. D., Ungaro, R. & Pochini, A. (1979). *J. Chem. Soc. Chem. Commun.* pp. 1005–1007.
- Brouwer, E. B., Enright, G. D., Ratcliffe, C. I. & Ripmeester, J. A. (1996). *Supramol. Chem.* **7**, 79–83.
- Facey, G. A., Dubois, R. H., Zakrzewski, M., Ratcliffe, C. I., Atwood, J. L. & Ripmeester, J. A. (1993). *Supramol. Chem.* **1**, 199–200.
- Gabe, E. J., Le Page, Y., Charland, J. P., Lee, F. L. & White, P. S. (1989). *J. Appl. Cryst.* **22**, 384–387.
- Le Page, Y. (1988). *J. Appl. Cryst.* **21**, 983–984.
- Sheldrick, G. M. (2001). *SHELXTL*. Bruker-AXS, Madison, Wisconsin, USA.